Sigma J Eng Nat Sci, Vol. 42, No. 1, pp. 189−197, February, 2024

Sigma Journal of Engineering and Natural Sciences
Web page info: https://sigma.yildiz.edu.tr
DOI: 10.14744/sigma.2022.00019

Research Article

Xerogel of fast kinetics and high adsorption capacity for cationic dye removal

Deniz SEZGİN[1], Müge Sarı YILMAZ[1,*]

[1]*Department of Chemical Engineering, Yıldız Technical University, Istanbul, 34220, Türkiye*

ARTICLE INFO

Article history
Received: 12 December 2021,
Revised: 18 January 2022
Accepted: 13 February 2022

Keywords:
Xerogel; Fast Kinetics; High Capacity; Adsorption; Cationic Dye

ABSTRACT

Silica-based xerogel was prepared by the two-step sol-gel method to investigate its methylene blue removal performance. The characteristics of the prepared adsorbent were determined using X-ray diffraction (XRD), Fourier transforms infrared (FTIR), scanning electron microscopy (SEM), and N_2 adsorption/desorption analyses. The MB removal studies were conducted with different operating parameters and optimal conditions were found to be 0.06 g adsorbent dosage, and 20 mg.L^{-1} initial MB concentration at 45 min. The Langmuir isotherm best represents the MB adsorption equilibrium data and the high maximum adsorption capacity was achieved with 1666.67 mg.g^{-1}. The kinetic mechanism of the study is defined by the pseudo-second-order kinetic model. Additionally, the adsorption of MB on xerogel exhibited fast kinetics, reaching a high removal capacity (96.56%) in a minute.

Cite this article as: Sezgin D, Yılmaz MS. Xerogel of fast kinetics and high adsorption capacity for cationic dye removal. Sigma J Eng Nat Sci 2024;42(1):189−197.

INTRODUCTION

It is estimated that approximately 100.000 various types of dye are used broadly in different fields including paper, textile, leather tanning, printing, cosmetics, and food processing for different purposes [1,2]. The discharge of generated dyestuff effluents from these fields into water resources without any treatment adversely affects the living life and disrupts the ecological system owing to their toxic and carcinogenic contents [3,4]. Furthermore, the effluents containing dyes decrease light penetration, thereby severely influencing the photosynthetic activity of aquatic livings [5].

Methylene blue (MB) is a cationic dye that is widely preferred as a colorant for cotton, wool, and silk [6]. MB appears considerably in industrial wastewater, and it is recognized that even its presence of much less than 1 ppm may also result in unfavorable impacts on the ecosystem balance [7,8]. Even though it is accepted that MB is not a highly harmful dye, long-term exposure to MB will induce eye irritation, heart rate increase, dizziness, headache, nausea, vomiting, and allergy [9,10]. Therefore, it is crucial to eliminate MB from effluent wastes before their discharge into water resources.

Up to the present, different treatment technologies have been developed including adsorption [9,11], electrochemical degradation [12], ion exchange [13], membrane filtration [14], and oxidation [15]. Compared with other removal techniques, adsorption is regarded as an appealing

***Corresponding author.**
*E-mail address: mugesari@yildiz.edu.tr

This paper was recommended for publication in revised form by Regional Editor Azmi Seyhun Kıpçak

Published by Yıldız Technical University Press, İstanbul, Turkey

approach in terms of its high yield, ease of design, and low process cost [16,17]. For this purpose, numerous adsorbents have been evaluated for the MB adsorption process such as silica-based materials [18–21], activated carbon [22], carbon nanotubes [23], graphene oxide [3,24], and zeolite [25]. Silica-based materials possess large pore volume, adjustable pore size, high mechanical, and thermal stabilities [26,27]. These materials with specific properties have broad applications in catalysis [28], thermal insulation [29], biomedical [30], and adsorption [20,31]. Silica xerogel is one of the silica-based materials frequently preferred in adsorption processes owing to its wide surface area, ease of synthesis, easy chemical functionality, and non-toxic properties in the environment [32,33]. In addition, the reported studies in the literature show that silica xerogel has achieved promising adsorption capacity in dye adsorption. Guzel Kaya et al. synthesized a silica xerogel from volcanic tuff with a high surface area and this material was used to examine its MB adsorption behavior. They observed that synthesized xerogel had a high MB removal capacity and good thermal stability [34]. Hannachi et al. fabricated a novel bi-functionalized xerogel for application as an adsorbent. They reported that the xerogel exhibited high adsorption capacity and regenerable function [35]. The mesoporous silica-based xerogel prepared by Mota et al. showed high MB removal capacity and large specific pore volumes [36].

To the best of the authors' knowledge, there are not many studies in the literature on the removal of methylene blue by xerogel synthesized from pure silica with a high adsorption capacity as in this study. In the present work, xerogel was synthesized according to the two-step sol-gel method and its MB adsorption performance was examined. For this purpose, removal studies were performed by various parameters (xerogel amount, time, and initial MB concentration). The obtained adsorption data were investigated by Langmuir and Freundlich isotherms. Also, the kinetic mechanism of adsorption was identified by conducting kinetic studies.

EXPERIMENTAL

Materials

Tetraethylorthosilicate (TEOS), ethanol, toluene, HCl, and MB were supplied from Sigma-Aldrich. Ammonia solution (NH_4OH, 25 wt%), was purchased from J.T. Baker.

XRD measurements were performed on a PANalytical X'Pert-Pro XRD diffractometer using CuKα radiation (40 kV, 40 mA). Infrared spectra were recorded over a spectral region from 4000 to 450 cm^{-1} using Perkin Elmer Spectrum One FT-IR spectrophotometer models accompanied with both KBr pellets. SEM images were recorded using Zeiss EVO®LS 10. The textural properties of the sample were determined on the Micromeritics ASAP 2020 adsorption device.

Synthesis of Xerogel

Silica xerogel was prepared according to the acid and base-catalyzed two-step sol-gel method previous study [37]. In the initial step, certain amounts of TEOS, ethanol, distilled water, and HCl were added in an Erlenmeyer flask. The mixture was exposed to the ultrasonic irradiation in an ultrasonic bath for 5 min and kept at 60 °C for 60 min to form a hydrolysis solution. In the second step, the mixture of the distilled water and NH_4OH was dropped in the hydrolysis solution and the obtained silica sol was kept at the ultrasonic bath for 5 min under ultrasonic irradiation. The sol was poured into a Teflon vessel and waited at 50 °C for gelation. The obtained gel was treated with ethanol four times at 50 °C and then the same washing process was repeated with toluene. The final gel was dried at 60 °C until it reaches a constant weight.

Adsorption Studies

MB aqueous solutions of various concentrations (10 to 100 mg.L^{-1}) were prepared to examine the initial dye concentration effect on silica-based xerogel adsorption. The effects of xerogel amount, contact time, and initial MB concentration on the dye removal efficiency of silica-based xerogel were investigated in the adsorption study. Firstly, the study of the xerogel amount effect on adsorption was carried out by adding various sample dosages starting from 0.02 to 0.25 g to each Erlenmeyer flasks containing 50 mL MB solution. The Erlenmeyer flasks containing dye-adsorbent mixture were shaken for 1 h at 25 °C using a shaking incubator. At the end of the time, the mixtures were filtered and the dye concentrations in the obtained filtrates were measured by an UV-visible spectrophotometer (Perkin Elmer, Lambda 35).

The effects of the other parameters on the adsorption of xerogel were carried out via a similar procedure. In each run, the determined content of xerogel was added to Erlenmeyer flasks including 50 mL of a given concentration of MB aqueous solution. The amount of adsorbed MB by xerogel at equilibrium (q_e) and the adsorption efficiency ($AE\%$) were found by applying the following equations;

$$q_e = \frac{V.(C_0 - C_e)}{M} \tag{1}$$

$$AE\% = \left(\frac{C_0 - C_e}{C_0}\right).100 \tag{2}$$

where C_0 and C_e are the initial and equilibrium concentrations of MB (mg.L^{-1}), respectively. M is the amount of xerogel used (g) and V is the volume of the MB solution (L) [38].

RESULTS AND DISCUSSION

Characterization

The XRD pattern of the silica-based xerogel was presented in figure. As shown in Figure 1, the synthesized sample demonstrates a broad peak between 20° and 30°. The broadness of this peak is typical of the silica-based sample with an amorphous structure [39].

The FT-IR spectrum of the produced silica-based xerogel was depicted in Figure 2. The broadband at 3448 cm^{-1} was related to -OH group stretching vibration. The peaks at 467, 797, and 1087 cm^{-1} corresponded to the bending, symmetric, and asymmetric vibrations arising from Si-O-Si, respectively. Furthermore, the vibration of H-O-H showing the presence of H_2O molecules was observed at 1636 cm^{-1}. The Si-OH vibration appeared at 946 cm^{-1}. In the meantime, Si-O stretching of O-Si-O network defects was observed at 569 cm^{-1} [19,39–41].

The surface area, the total pore volume, and the average pore width of xerogel was 375.86 $m^2.g^{-1}$, 0.28 $cm^3.g^{-1}$, and 3.69 nm, respectively. The SEM image of the sample was given in Figure 3. It is seen that the sample has small and agglomerated particles in non-uniform shape. The porous structure could not be seen clearly due to the low resolution of SEM.

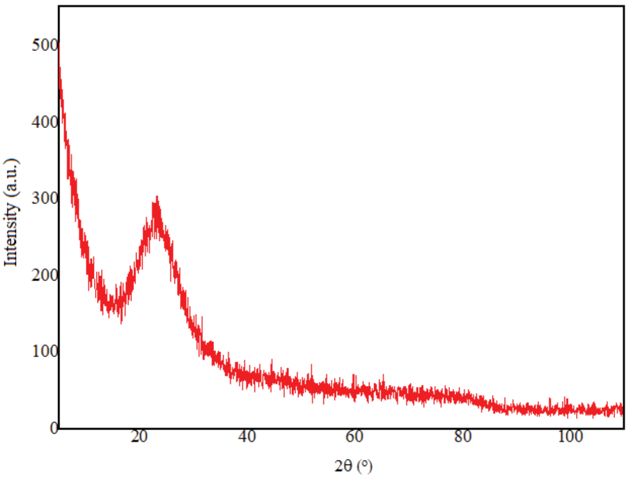

Figure 1. XRD pattern of silica-based xerogel.

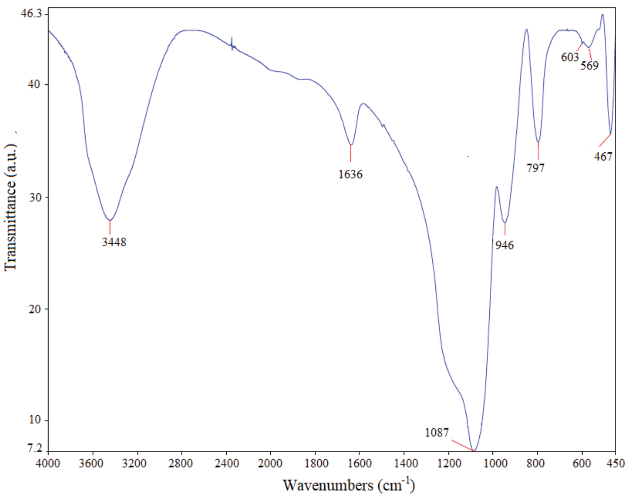

Figure 2. FT-IR spectrum of adsorbent.

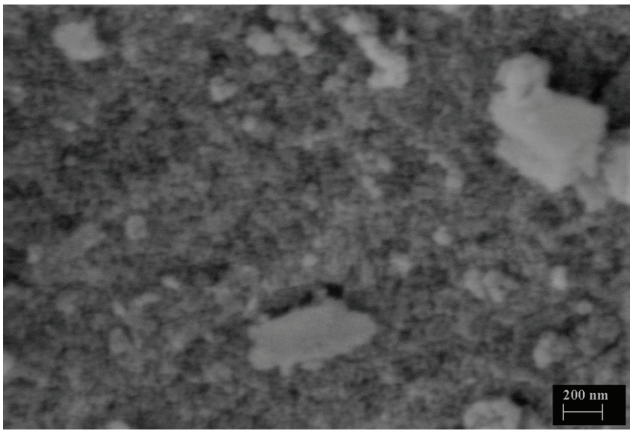

Figure 3. SEM image of silica-based xerogel.

Effect of Xerogel Amount

The relationship between the varied dose of adsorbent (0.02-0.25 g) and adsorption efficiency was investigated by keeping the other parameters stable. According to Figure 4a, the removal rate increased quickly up to 0.02 g, and then slowly reached equilibrium at 0.06 g. The constant uptake capacity of xerogel after equilibrium may result from the reduction of the total surface area of MB adsorption due to aggregation or overlapping of adsorption sites [43]. It was obtained that the optimum dose of adsorbent providing the highest efficiency (99.4%) was found as 0.06 g.

Effect of Time

The contact time effect on the MB removal efficiency of xerogel was conducted at predetermined various times starting from 1 to 120 min by using the adsorbent amount of 0.06 g and dye concentration of 20 $mg.L^{-1}$. Figure 4b demonstrated the variation of adsorption efficiency depending on the time. In the figure, the adsorption of MB onto xerogel increased rapidly within 1 min, and then a slight increase was observed up to 45 min. After 45 min, it approached nearly a constant value and at this time the adsorption efficiency of the xerogel was observed as 98.4%.

Effect of Initial Concentration

The MB concentration effect on adsorption capacity was determined by selecting different concentration ranges (10-100 $mg.L^{-1}$). As given in Figure 4c, the removal efficiency of dye increased instantly until 10 $mg.L^{-1}$ and a considerable increment was not seen between 10 and 20 $mg.L^{-1}$. After reaching equilibrium, the uptake capacity of xerogel gradually decreased with increasing MB concentration. The highest amount of MB removal was measured at 20 $mg.L^{-1}$ with 99.65%.

Adsorption Kinetics

Pseudo-first order (*PFOM*) and pseudo-second order (*PSOM*) kinetic models were employed to analyze the kinetics of the adsorption study. The *PFOM* and the *PSOM* were stated as Eqs. 3 and 4, respectively [44];

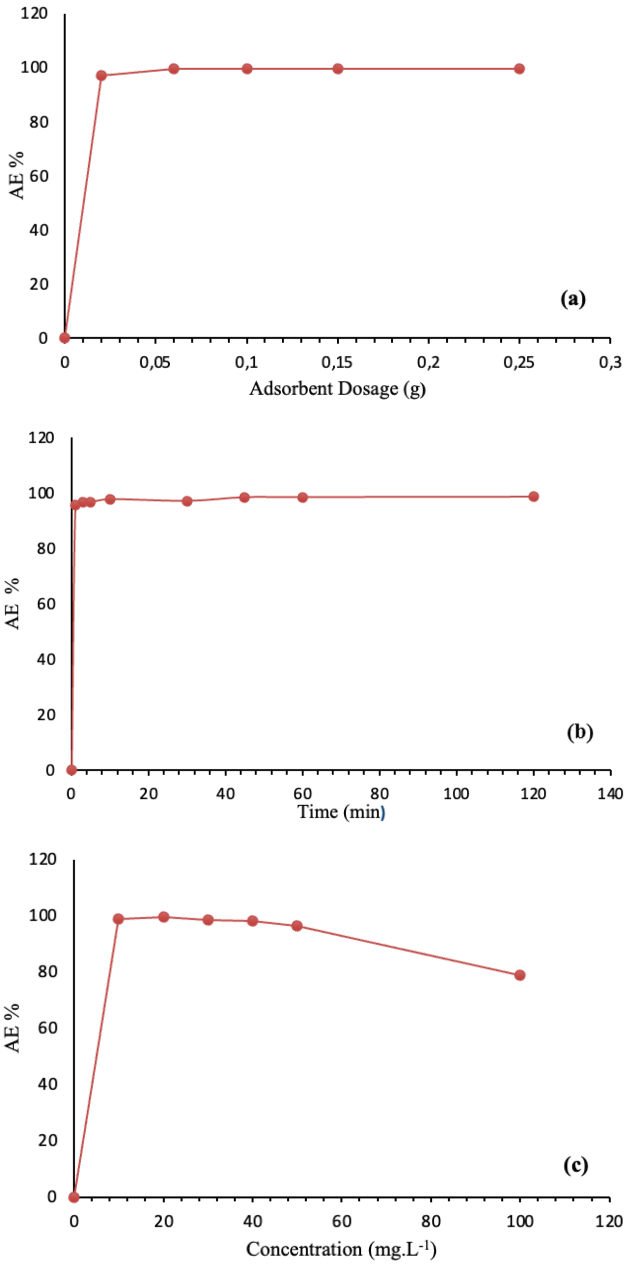

Figure 4. Effect of various parameters on the adsorption of MB (a) Adsorbent dosage, (b) Time, and (c) Initial concentration.

$$ln(q_e - q_t) = ln(q_e) - k_1 t \tag{3}$$

$$\frac{t}{q_t} = \frac{1}{k_2 q_e^2} + \frac{t}{q_e} \tag{4}$$

where q_e is the amount of MB adsorption by the silica-based xerogel at equilibrium, while q_t is the adsorbed MB amount at time *t*. Also, k_1 and k_2 represent the rate constants of *PFOM* and *PSOM*.

Table 1. Kinetic parameters for the *PFOM* and *PSOM*

	PFOM			*PSOM*		
$q_{e,exp}$	q_e	k_1	R^2	q_e	k_2	R^2
18.523	2.903	0.0178	0.1801	18.553	0.403	1

The drawn plots of *PFOM* and *PSOM* were given in Figure 5. The estimated parameters and regression coefficients (R^2) were presented in Table 1. It was seen that the calculated R^2 in the *PSOM* was considerably higher than that found in the *PFOM*. Additionally, the q_e value estimated by *PSOM* and the q_e value obtained experimentally were found to be almost the same. Hence, it can be stated that the *PSOM* best expresses the kinetic mechanism of the MB adsorption study.

Adsorption Isotherm

The estimation of isotherm data is necessary to explain the adsorption ability of the adsorbent [38]. In the present work, the Langmuir (*LM*) and Freundlich (*FM*) isotherm models were employed to analyze the obtained equilibrium data of MB adsorption onto silica-based xerogel. The expressions of the *LM* and FM were presented in Eqs. 5 and 6, respectively [45];

$$\frac{C_e}{q_e} = \frac{1}{q_m K_L} + \frac{C_e}{q_m} \tag{5}$$

$$ln\, q_e = ln\, K_f + \frac{1}{n} ln\, C_e \tag{6}$$

where C_e is MB concentration at equilibrium (mg.L^{-1}), q_e is the adsorbed MB dosage at equilibrium (mg.g^{-1}), q_m is the maximum adsorption capacity of the silica-based xerogel (mg.g^{-1}). K_L and K_f are calculated from the intercept of the graphs given in Figure 6a and b, respectively and *n* is a constant found as the slope of Figure 6b.

The calculated parameters and correlation coefficients (R^2) of *LM* and *FM* were depicted in Table 2. It was found that the experimental data received from MB adsorption fitted to the *LM* in comparison to *FM* in terms of correlation coefficients. The fact that the *LM* conforms quite well with the equilibrium data shows that the process occurs over a homogeneous surface using single-layer sorption [38]. The maximum adsorption capacity (q_m) of the study was found as 1666.67 mg.g^{-1}, and it was compared with previously reported silica-based adsorbents presented in Table 3. The xerogel had the greatest adsorption capacity among all the silica-based adsorbents. Therefore, xerogel can be applied as an

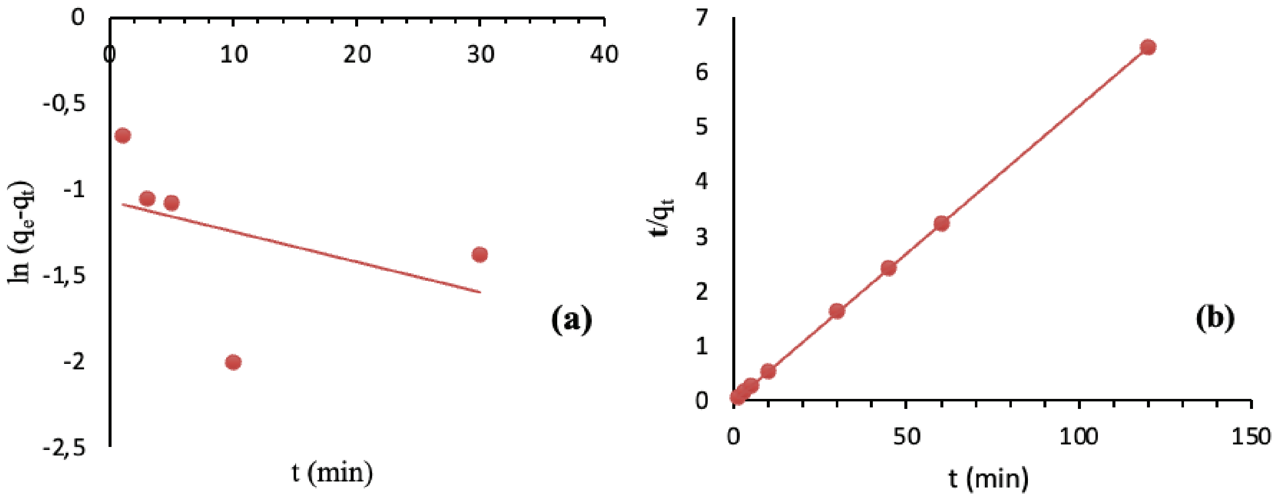

Figure 5. The MB adsorption kinetics plots (a) *PFOM* and (b) *PSOM*. Experimental conditions: dosage of the adsorbent: 0.06 g and initial dye concentration: 20 mg.L^{-1}.

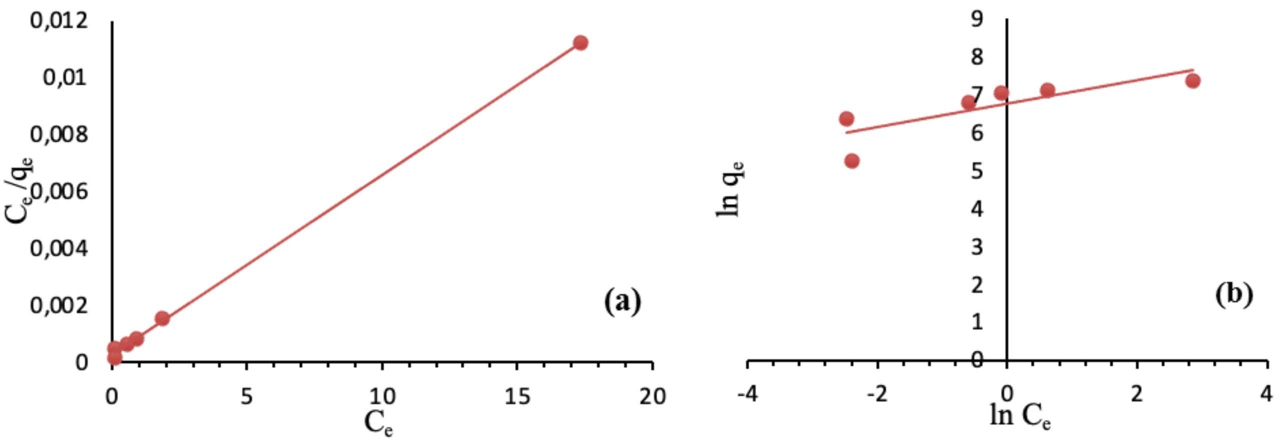

Figure 6. (a) *LM* and (b) *FM* model plots. Experimental conditions: dosage of the adsorbent: 0.06 g and time: 45 min.

Table 2. Isotherm parameters for the adsorption of MB on the sample

Langmuir			**Freundlich**		
q_m **(mg.g^{-1})**	K_L **(L.mg^{-1})**	R^2	K_F **(mg.g^{-1})**	n **(L.mg^{-1})**	R^2
1666.67	2	0.9993	857.31	3.22	0.6714

effective adsorbent for the removal of MB dye over other available adsorbents.

The characteristics of adsorption isotherm can be analyzed using separation factor (r_L) that was expressed by Eq. 7;

$$r_L = \frac{1}{1+(K_L C_0)} \quad (7)$$

where K_L is the *LM* constant (L.mg^{-1}) and C_0 is the highest initial MB concentration (mg.L^{-1}). The separation factor in the current study was calculated as 0.0244 ($0<r_L<1$), showing that the MB removal process of silica-based xerogel is favorable [22].

Table 3. Maximum MB adsorption capacities (q_m) of silica-based materials from the cited in literature

Adsorbent	q_m (mg.g^{-1})	Reference
$MgFe_2O_4$@SiO_2 NPs	4.98	[8]
Fe_3O_4@SiO_2-CR	63.69	[17]
$nSiO_2$	547.5	[19]
MW–$nSiO_2$	679.9	[19]
(MAA-co-MMA)/SiO_2	85.33	[46]
(MAA-co-HPMA)/SiO_2	87.37	[46]
HSA	47.211	[47]
MSA	65.746	[47]
SBA-12-OH	91.1	[48]
Silica-chitosan-ZnO Nanocomposite	293.3	[49]
Silica Nanoparticles	347.2	[50]
Silica Nanoparticles	113.636	[51]
Silica Nanoparticles	511.04	[52]
Silica Nanoparticles	500.1	[53]
Silica Nanoparticles	380	[54]
Silica Nanoparticles	375.9	[55]
SiO_2/CA	1158.332	[56]
Hollow Silica Nanoparticles	64.06	[57]
GO/Hollow Mesoporous Silica	476.19	[24]
Cyclodextrin/Silica	212	[58]
mwXG-g-PANi/SiO_2	1250	[59]
Silica Xerogel	51.967	[34]
Silica Xerogel	512	[35]
Silica Xerogel	1666.67	This work

CONCLUSION

In the present work, silica-based xerogel was synthesized and utilized as an adsorbent for MB adsorption at different operating parameters. The obtained results exhibited that the MB adsorption process depends on the amount of xerogel, time, and initial MB concentration. The highest removal capacity of xerogel was reached at 45 min with 20 mg.L^{-1} initial MB concentration, and 0.06 g of xerogel. The high removal capacity of xerogel reached within 1 min indicates that the adsorption of MB is fast. The *PSOM* with a high R^2 represents well the kinetic mechanism of the study. The *LM* isotherm fitted best the obtained equilibrium data and achieved maximum adsorption capacity (1666.67 mg.g^{-1}) can be assigned as quite high when compared to MB adsorption studies with silica-based materials. It can be stated that silica-based xerogel is an appropriate adsorbent for the elimination of MB from aqueous solution, owing to its high yield, great adsorbing capacity, and fast process.

NOMENCLATURE

AE	Adsorption efficiency
C_0	Initial concentrations of MB, mg.L^{-1}
C_E	Equilibrium concentrations of MB, mg.L^{-1}
k_1	Pseudo-first order model constant
k_2	Pseudo-second order model constant
K_L	Langmuir isotherm model constant
K_f	Freundlich isotherm model constant
M	The amount of xerogel, g
r_L	Separation factor
q_e	The amount of adsorbed MB by xerogel at equilibrium, mg.g^{-1}
q_m	The maximum adsorption capacity of the silica-based xerogel, mg.g^{-1}
q_t	The amount of adsorbed MB by xerogel at time *t*, mg.g^{-1}
V	Volume of the MB solution, L

AUTHORSHIP CONTRIBUTIONS

Authors equally contributed to this work.

DATA AVAILABILITY STATEMENT

The authors confirm that the data that supports the findings of this study are available within the article. Raw data that support the finding of this study are available from the corresponding author, upon reasonable request.

CONFLICT OF INTEREST

The author declared no potential conflicts of interest with respect to the research, authorship, and/or publication of this article.

ETHICS

There are no ethical issues with the publication of this manuscript.

REFERENCES

[1] Crini G. Non-conventional low-cost adsorbents for dye removal: A review. Bioresour Technol 2006;97:1061−1085. [CrossRef]

[2] Konicki W, Aleksandrzak M, Moszyński D, Mijowska E. Adsorption of anionic azo-dyes from aqueous solutions onto graphene oxide: Equilibrium, kinetic and thermodynamic studies. J Colloid Interface Sci 2017;496:188−200. [CrossRef]

[3] Li Y, Du Q, Liu T, Sun J, Wang Y, Wu S, et al. Methylene blue adsorption on graphene oxide/calcium alginate composites. Carbohydr Polym 2013;95:501−507. [CrossRef]

[4] Yagub MT, Sen TK, Afroze S, Ang HM. Dye and its removal from aqueous solution by adsorption: A review. Adv Colloid Interface Sci 2014;209:172−184. [CrossRef]

[5] Chen Z, Fu J, Wang M, Wang X, Zhang J, Xu Q. Adsorption of cationic dye (methylene blue) from aqueous solution using poly(cyclotriphosphazene-co-4,4′-sulfonyldiphenol) nanospheres. Appl Surf Sci 2014;289:495−501. [CrossRef]
[6] Zhang W, Zhang LY, Zhao XJ, Zhou Z. Citrus pectin derived ultrasmall Fe3O4@C nanoparticles as a high-performance adsorbent toward removal of methylene blue. J Mol Liq 2016;222:995−1002. [CrossRef]
[7] Ravi, Pandey LM. Enhanced adsorption capacity of designed bentonite and alginate beads for the effective removal of methylene blue. Appl Clay Sci 2019;169:102−111. [CrossRef]
[8] Hoijang S, Wangkarn S, Ieamviteevanich P, Pinitsoontorn S, Ananta S, Lee TR, et al. Silica-coated magnesium ferrite nanoadsorbent for selective removal of methylene blue. Colloids Surf A Physicochem Eng Asp 2020;606:125483. [CrossRef]
[9] Xiao X, Zhang F, Feng Z, Deng S, Wang Y. Adsorptive removal and kinetics of methylene blue from aqueous solution using NiO/MCM-41 composite. Phys E: Low-dimens Syst Nanostructures 2015;65:4−12. [CrossRef]
[10] Hassan AF, Abdel-Mohsen AM, Fouda MM. Comparative study of calcium alginate, activated carbon, and their composite beads on methylene blue adsorption. Carbohydr Polym 2014;102:192−198. [CrossRef]
[11] Chen J, Feng J, Yan W. Influence of metal oxides on the adsorption characteristics of PPy/metal oxides for Methylene Blue. J Colloid Interface Sci 2016;475:26−35. [CrossRef]
[12] Panizza M, Barbucci A, Ricotti R, Cerisola G. Electrochemical degradation of methylene blue. Sep Purif Technol 2007;54:382−387. [CrossRef]
[13] Labanda J, Sabaté J, Llorens J. Experimental and modeling study of the adsorption of single and binary dye solutions with an ion-exchange membrane adsorber. Chem Eng J 2011:166:536−543. [CrossRef]
[14] Soniya M, Muthuraman G. Comparative study between liquid-liquid extraction and bulk liquid membrane for the removal and recovery of methylene blue from wastewater. J Ind Eng Chem 2015;30:266−273. [CrossRef]
[15] Salem IA, El-Maazawi MS. Kinetics and mechanism of color removal of methylene blue with hydrogen peroxide catalyzed by some supported alumina surfaces. Chemosphere 2000;41:1173−1180. [CrossRef]
[16] Bazrafshan AA, Ghaedi M, Hajati S, Naghiha R, Asfaram A. Synthesis of ZnO-nanorod-based materials for antibacterial, antifungal activities, DNA cleavage and efficient ultrasound-assisted dyes adsorption. Ecotoxicol Environ Saf 2017;142:330−337. [CrossRef]
[17] Yimin D, Jiaqi Z, Danyang L, Lanli N, Liling Z, Yi Z, et al, Preparation of Congo red functionalized Fe3O4@SiO2 nanoparticle and its application for the removal of methylene blue. Colloids Surf A Physicochem Eng Asp 2018;550:90−98. [CrossRef]
[18] Diagboya PNE, Dikio ED. Silica-based mesoporous materials; emerging designer adsorbents for aqueous pollutants removal and water treatment. Microporous Mesoporous Mater 2018;266:252−267. [CrossRef]
[19] Peres EC, Slaviero JC, Cunha AM, Hosseini-Bandegharaei A, Dotto G. Microwave synthesis of silica nanoparticles and its application for methylene blue adsorption. J Environ Chem Eng 2018;6:649−659. [CrossRef]
[20] Sheng L, Zhang Y, Tang F, Liu S. Mesoporous/microporous silica materials: Preparation from natural sands and highly efficient fixed-bed adsorption of methylene blue in wastewater. Microporous Mesoporous Mater 2018;257:9−18. [CrossRef]
[21] Erturk S, Sari Yilmaz M, Piskin S. Potential low-cost carbon-based adsorbent from gold mine tailings for anionic dye removal. Water Sci Technol 2021;83:1300−1314. [CrossRef]
[22] Hameed BH, Din AT, Ahmad AL. Adsorption of methylene blue onto bamboo-based activated carbon: Kinetics and equilibrium studies. J Hazard Mater 2007;141:819−825. [CrossRef]
[23] Yao Y, Xu F, Chen M, Xu Z, Zhu Z. Adsorption behavior of methylene blue on carbon nanotubes. Bioresour Technol 2010;101:3040−3046. [CrossRef]
[24] Sari Yilmaz M. Graphene oxide/hollow mesoporous silica composite for selective adsorption of methylene blue. Microporous Mesoporous Mater 2022;330:111570. [CrossRef]
[25] Han R, Zhang J, Han P, Wang Y, Zhao Z, Tang M. Study of equilibrium, kinetic and thermodynamic parameters about methylene blue adsorption onto natural zeolite. Chem Eng J 2009;145:496−504. [CrossRef]
[26] Benvenuti J, Fisch A, dos Santos JHZ, Gutterres M. Silica-based adsorbent material with grape bagasse encapsulated by the sol-gel method for the adsorption of Basic Blue 41 dye. J Environ Chem Eng 2019;7:103342. [CrossRef]
[27] Rafatullah M, Sulaiman O, Hashim R, Ahmad A. Adsorption of methylene blue on low-cost adsorbents: A review. J Hazard Mater 2010;177:70−80. [CrossRef]
[28] Luque R, Balu AM, Campelo JM, Gracia MD, Losada E, Pineda A, et al. Catalytic applications of mesoporous silica-based materials. R Soc Chem 2012;43:253−280. [CrossRef]
[29] Karamahmut Mermer N, Sari Yilmaz M, Dere Ozdemir O, Piskin MB. The synthesis of silica-based aerogel from gold mine waste for thermal insulation. J Therm Anal Calorim 2017;129:1807−1812. [CrossRef]

[30] Knežević NŽ, Ruiz-Hernández E, Hennink WE, Vallet-Regí M. Magnetic mesoporous silica-based core/shell nanoparticles for biomedical applications. RSC Adv 2013;3:9584. [CrossRef]

[31] Pawlaczyk M, Schroeder G. Adsorption studies of Cu(II) ions on dendrimer-grafted silica-based materials. J Mol Liq 2019;281:176−185. [CrossRef]

[32] Sriram G, Uthappa UT, Madhuprasad K, Ho-Young J, Tariq A, Brahmkhatri Varsha P, et al. Xerogel activated diatoms as an effective hybrid adsorbent for the efficient removal of malachite green. New J Chem 2019;43:3810−3820. [CrossRef]

[33] Osagie C, Othmani A, Ghosh S, Malloum A, Kashitarash Esfahani Z, Ahmadi S. Dyes adsorption from aqueous media through the nanotechnology: A review. J Mater Res Technol 2021;14:2195−2218. [CrossRef]

[34] Guzel Kaya G, Yilmaz E, Deveci H. A novel silica xerogel synthesized from volcanic tuff as an adsorbent for high-efficient removal of methylene blue: Parameter optimization using Taguchi experimental design. J Chem Technol Biotechnol 2019;94:2729−2737. [CrossRef]

[35] Hannachi Y, Hafidh A. Preparation and characterization of novel bi-functionalized xerogel for removal of methylene blue and lead ions from aqueous solution in batch and fixed-bed modes: RSM optimization, kinetic and equilibrium studies. J Saudi Chem Soc 2020;24:505−519. [CrossRef]

[36] Mota TLR, Gomes ALM, Palhares HG, Nunes EHM, Houmard M. Influence of the synthesis parameters on the mesoporous structure and adsorption behavior of silica xerogels fabricated by sol-gel technique. J Sol-Gel Sci Technol 2019;92:681−694. [CrossRef]

[37] Venkateswara Rao A, Nilsen E, Einarsrud MA. Effect of precursors, methylation agents and solvents on the physicochemical properties of silica aerogels prepared by atmospheric pressure drying method. J Non Cryst Solids 2001;296:165−171. [CrossRef]

[38] Ali RM, Hamad HA, Hussein MM, Malash GF. Potential of using green adsorbent of heavy metal removal from aqueous solutions: Adsorption kinetics, isotherm, thermodynamic, mechanism and economic analysis. Ecol Eng 2016;91:317−332. [CrossRef]

[39] Hu W, Li M, Chen W, Zhang N, Li B, Wang M, et al. Preparation of hydrophobic silica aerogel with kaolin dried at ambient pressure. Colloids Surf A Physicochem Eng Asp 2016;501:83−91. [CrossRef]

[40] Al-Oweini R, El-Rassy H. Synthesis and characterization by FTIR spectroscopy of silica aerogels prepared using several Si(OR)4 and R′′Si(OR′)3 precursors. J Mol Struct 2009;919:140−145. [CrossRef]

[41] Standeker S, Novak Z, Knez Z. Adsorption of toxic organic compounds from water with hydrophobic silica aerogels. J Colloid Interface Sci 2007;310:362−368. [CrossRef]

[42] Li M, Jiang H, Xu D, Hai O, Zheng W. Low density and hydrophobic silica aerogels dried under ambient pressure using a new co-precursor method. J Non Cryst Solids 2016;452:187−193. [CrossRef]

[43] Crini G, Peindy H, Gimbert F, Robert C. Removal of C.I. Basic Green 4 (Malachite Green) from aqueous solutions by adsorption using cyclodextrin-based adsorbent: Kinetic and equilibrium studies. Sep Purif Technol 2007;53:97−110. [CrossRef]

[44] Chairat M, Rattanaphani S, Bremner JB, Rattanaphani V. Adsorption kinetic study of lac dyeing on cotton. Dyes Pigm 2008;76:435−439. [CrossRef]

[45] Hameed BH, Salman JM, Ahmad AL. Adsorption isotherm and kinetic modeling of 2,4-D pesticide on activated carbon derived from date stones. J Hazard Mater 2009;163:121−126. [CrossRef]

[46] Jamwal HS, Kumari S, Chauhan GS, Reddy NS, Ahn JH. Silica-polymer hybrid materials as methylene blue adsorbents. J Environ Chem Eng 2017;5:103−113. [CrossRef]

[47] Han H, Wei W, Jiang Z, Lu J, Zhu J, Xie J. Removal of cationic dyes from aqueous solution by adsorption onto hydrophobic/hydrophilic silica aerogel. Colloids Surf A Physicochem Eng Asp 2016;509:539−549. [CrossRef]

[48] Ge S, Geng W, He X, Zhao J, Zhou B, Duan L, et al. Effect of framework structure, pore size and surface modification on the adsorption performance of methylene blue and Cu2+ in mesoporous silica. Colloids Surf A Physicochem Eng Asp 2018;539:154−162. [CrossRef]

[49] Hassan H, Salama A, El-Ziaty AK, El-Sakhawy M. New chitosan/silica/zinc oxide nanocomposite as adsorbent for dye removal. Int J Biol Macromol 2019;131:520−526. [CrossRef]

[50] Yu ZH, Zhai SR, Guo H, Iv TM, Song Y, Zhang F, et al. Removal of methylene blue over low-cost mesoporous silica nanoparticles prepared with naturally occurring diatomite. J Sol Gel Sci Technol 2018;88:541−550. [CrossRef]

[51] Dhmees AS, Khaleel NM, Mahmoud SA. Synthesis of silica nanoparticles from blast furnace slag as cost-effective adsorbent for efficient azo-dye removal. Egypt J Pet 2018;27:1113−1121. [CrossRef]

[52] Li Z, Sellaoui L, Gueddida S, Dotto G, Lamine AB, Badawi M, et al. Adsorption of methylene blue on silica nanoparticles: Modelling analysis of the adsorption mechanism via a double layer model. J Mol Liq 2020;319:114348. [CrossRef]

[53] Karim AH, Triwahyono S, Sidik SM, Kamarudin NHN, Jusoh R, Jusoh NWC, et al. Amino modified mesostructured silica nanoparticles for efficient adsorption of methylene blue. J Colloid Interface Sci 2012;386:307−314. [CrossRef]

[54] Parida D, Salmeia KA, Sadeghpour A, Zhao S, Maurya AK, Assaf KI, et al. Template-free synthesis

of hybrid silica nanoparticle with functionalized mesostructure for efficient methylene blue removal. Mater Des 2021;201:109494. [CrossRef]

[55] Saleh TA, Al-Ruwayshid SH, Sarı A, Tuzen M. Synthesis of silica nanoparticles grafted with copolymer of acrylic acrylamide for ultra-removal of methylene blue from aquatic solutions. Eur Polym J 2020;130:109698. [CrossRef]

[56] Shi J, Zhang H, Yu Y, Zou X, Zhou W, Guo J, et al. Adsorption Properties of calcium alginate-silica dioxide hybrid adsorbent to methylene blue. J Inorg Organomet Polym Mater 2020;30:2114–2125. [CrossRef]

[57] Verma M, Dwivedi PK, Saxena NS. Hollow silica nanoparticles synthesized from core-shell nanoparticles as highly efficient adsorbent for methylene blue and its invitro release: Mechanism and Kinetics study. Colloids Surf A Physicochem Eng Asp 2020;587:124333. [CrossRef]

[58] Carvalho LB, Carvalho TG, Magriotis ZM, Ramalho TDC, Pinto LDMA. Cyclodextrin/silica hybrid adsorbent for removal of methylene blue in aqueous media. J Incl Phenom Macrocycl Chem 2014;78:77–87. [CrossRef]

[59] Sadanand S, Fosso-Kankeu E, Ramontja J. Efficient and Rapid Adsorption Characteristics of Templating Xanthan Gum-Graft-Poly (Aniline) and Silica Nanocomposite toward Removal of Toxic Methylene Blue Dyes. In: 9th Int'l Conference on Advances in Science, Engineering, Technology & Waste Management (ASETWM-17). 2017.